

1 Simulated effects of southern hemispheric wind 2 changes on the Pacific oxygen minimum zone

Julia Getzlaff¹, Heiner Dietze¹ and Andreas Oschlies^{1,2}

J. Getzlaff, GEOMAR Helmholtz Centre for Ocean Research Kiel, Germany. (jgetzlaff@geomar.de)

H. Dietze, GEOMAR Helmholtz Centre for Ocean Research Kiel, Germany.

A. Oschlies, GEOMAR Helmholtz Centre for Ocean Research Kiel and Kiel University, Germany

¹GEOMAR Helmholtz Centre for Ocean Research Kiel, Kiel, Germany.

²Kiel University, Germany.

This article has been accepted for publication and undergone full peer review but has not been through the copyediting, typesetting, pagination and proofreading process which may lead to differences between this version and the Version of Record. Please cite this article as doi: 10.1002/2015GL066841

D B A F T December 28, 2015 9:16am D B A F T

3 A coupled ocean biogeochemistry-circulation model is used to investigate
4 the impact of observed past and anticipated future wind changes in the south-
5 ern hemisphere on the oxygen minimum zone in the tropical Pacific. We con-
6 sider the industrial period until the end of the 21st century and distinguish
7 effects due to a strengthening of the westerlies from effects of a southward
8 shift of the westerlies that is accompanied by a poleward expansion of the
9 tropical trade winds. Our model results show that a strengthening of the west-
10 erlies counteracts part of the warming-induced decline in the global marine
11 oxygen inventory. A poleward shift of the trade-westerlies boundary, how-
12 ever, triggers a significant decrease of oxygen in the tropical oxygen mini-
13 mum zone. In a business-as-usual CO₂ emission scenario, the poleward shift
14 of the trade-westerlies boundary and warming-induced increase in stratifi-
15 cation contribute equally to the expansion of suboxic waters in the tropical
16 Pacific.

1. Introduction

17 Oxygen is a sensitive indicator for physical and biological changes in the ocean. Its
18 supply can be affected by changes in surface temperature and circulation. The solubil-
19 ity of oxygen decreases as temperature rises, so that warming alone would result in a
20 decline of the global oxygen inventory with time. A decrease in oxygen levels has been
21 observed during the past decades [e.g. Stramma et al., 2012a], in particular in the trop-
22 ical oceans including the oxygen minimum zone (OMZ) of the eastern equatorial Pacific
23 (EEP). Changes in solubility can, however, explain only about a quarter of the observed
24 oxygen decline [Bopp et al., 2002]. The reminder has to be explained by changes in
25 physical transport or biological source-sink processes.

26 Global warming tends to enhance stratification and also affects wind patterns, which
27 both can alter the ventilation of the thermocline, biological production and, eventually,
28 respiration and oxygen consumption. Until now the contributions of the individual pro-
29 cesses to the observed oxygen decline are not well understood. In addition, the presence
30 of decadal atmospheric variability, such as the Pacific Decadal Oscillation [Deutsch et al.,
31 2014], makes it further difficult to detect the attribution of long-term trends. Improving
32 our mechanistic understanding of past and present oxygen variations is a major challenge
33 for making reliable projections of how tropical oxygen levels may evolve in the future.

34 Model simulations allow a straightforward investigation of the individual processes that
35 may lead to changes in marine oxygen fields. Previous simulations that employed clima-
36 tological winds and only applied a CO₂ dependent increase in temperature and buoyancy
37 forcing, consistently showed a decrease of the global oxygen inventory with time [Oschlies

38 et al., 2008]. They failed, however, to reproduce the observed patterns of oxygen changes
39 and in particular the observed decrease in the tropical thermocline [Dietze and Loeptien,
40 2013; Oschlies et al., 2008; Stramma et al., 2012a]. Stramma et al. [2012a] showed that
41 simulated oxygen changes in the tropical thermocline are very sensitive to the choice of the
42 applied wind stress forcing. The potential impact of changes in the tropical trade winds
43 has been investigated recently by Ridder et al. [2014], who found a direct correlation
44 between changes in the strength of the trade winds and the spatial extent of the OMZ.
45 This agrees with Duteil et al. [2014] who suggest that the strength of the wind-driven
46 subtropical-tropical cells is closely correlated with thermocline oxygen levels in the EEP.

47 While these studies focussed on impacts of local wind changes on oxygen levels in
48 the tropical thermocline, we here investigate the potential role of remote wind forcing:
49 Observation-based atmospheric reanalysis products indicate a strengthening and a pole-
50 ward shift of the southern westerly winds since the 1970s [Thompson and Solomon, 2002].
51 This is in line with an observed shift of the southern annular mode (SAM) towards a
52 higher index state [Thompson and Solomon, 2002; Marshall, 2003]. Regarding impacts on
53 the ocean, Saenko et al. [2005] show that an increase and poleward shift of the westerlies
54 result in a more intense meridional overturning circulation (MOC) in the southern hemi-
55 sphere. This is accompanied by a poleward expansion of the subtropical gyre circulation
56 and a strengthening of the Antarctic Circumpolar Current (ACC). Roemmich et al. [2007]
57 describe an observed intensification of the South Pacific subtropical gyre and suggest a
58 link to changes in the mid-latitude winds in response to a decadal or longer-term increase
59 in the SAM. The intensification of the Southern Ocean wind stress curl between the 1970s

60 and early 2000s has also been related to the observed strengthening of the southward East
61 Australian Current and of the northward interior transport [Cai, 2006]. Changes in the
62 subtropical gyre circulation may not only affect the western Pacific boundary currents
63 [e.g. Ridgway and Hill, 2009], but also the eastern Pacific boundary currents along with
64 the water mass transport into the OMZ of the EEP.

65 In this study we go beyond wind-induced impacts on ocean physics and evaluate the im-
66 pact of southern hemispheric wind changes on marine oxygen distributions. In particular,
67 we distinguish the effect of wind changes within the zonal band of the westerlies from wind
68 changes in the entire southern hemisphere that also include a poleward expansion of the
69 tropical trade winds. We hypothesize that changes in the strength of the westerlies mainly
70 affect the MOC and consequently the water mass formation rates of southern hemispheric
71 intermediate waters and mode waters. Changes in the meridional extension of the trade
72 winds, on the other hand, are expected to affect the subtropical gyre circulation and, in
73 turn, the ventilation of the subtropical thermocline and the associated oxygen supply to
74 the OMZ.

75 The paper is organized as follows: Section 2 describes the numerical model and the
76 experiments performed. In section 3, we discuss the model results and section 4 provides
77 a summary and conclusions.

2. Model

78 We use the University of Victoria (UVic) Earth System Climate model [Weaver et
79 al., 2001] version 2.9. The model includes a global three-dimensional primitive-equation
80 ocean model [Pacanowski, 1995], a single-level atmospheric energy-moisture balance model

D R A F T

December 28, 2015, 9:16am

D R A F T

81 [based on Fanning and Weaver, 1996], a dynamic-thermodynamic sea ice model, a marine
82 ecosystem model [Keller et al., 2012] and a terrestrial vegetation and carbon cycle model.
83 All model components use a horizontal resolution of 1.8° latitude \times 3.6° longitude. The
84 vertical grid of the oceanic component has 19 z-levels with a surface thickness of 50 m
85 increasing to 500 m at depth.

86 The ocean model includes isopycnal mixing and the Gent and McWilliams [1990] pa-
87 rameterization of eddy-induced tracer transport. It is coupled to the atmospheric energy-
88 moisture balance model and to the dynamic-thermodynamic sea ice model. The spin-up
89 time is 11,000 years until equilibrium is reached under preindustrial atmospheric CO_2 . A
90 detailed description of the model configuration is given in Keller et al. [2012].

91 In all experiments we employ a background isopycnal diffusion coefficient of $1200 \text{ m}^2 \text{ s}^{-1}$
92 and additionally use the parameterization of the unresolved equatorial current system as
93 described in Getzlaff and Dietze [2013] where the zonal (anisotropic) isopycnal diffusion
94 coefficient is increased by $50\,000 \text{ m}^2 \text{ s}^{-1}$ in the equatorial region between 5°S and 5°N .
95 This parameterisation improves the global representation of temperature, salinity and
96 oxygen by reducing spurious tracer gradients in the equatorial Pacific. This yields a more
97 realistic representation of tropical oxygen distributions, including the patterns of low oxy-
98 gen environments. The standard model configuration is forced by monthly climatological
99 NCAR/NCEP wind stress fields.

100 In all experiments, we apply anthropogenic CO_2 emissions according to the RCP 8.5
101 business-as-usual scenario. For diagnostic purposes, an ideal age tracer and three wa-
102 ter mass tracers were implemented that trace the pathways of Subantarctic mode water

103 (SAMW), Antarctic intermediate water (AAIW) and Antarctic bottom water (AABW)
104 in our model. The three artificial tracers are continuously set to values of 1 in the surface
105 layer between 41.4°S and 52.2°S, 52.2°S and 66.6°S, and south of 66.6°S, respectively.
106 Outside their respective release sites the tracers are reset to zero in the surface layer. The
107 meridional bounds are based on pragmatic reasoning and are chosen to ensure that the
108 respective water mass formation regions are comprised throughout the transient simula-
109 tions.

110 In the reference simulation, REF, monthly climatological NCAR/NCEP wind forcing
111 is applied. In the first sensitivity study, WIND, we add a 300-year record of monthly
112 meridional and zonal wind stress anomalies in the southern hemisphere to the monthly
113 climatology. The wind stress anomalies (see Figure 1 a) are the same as used by Spence
114 et al. [2010] and described in greater detail in Fyfe et al. [2007]. These monthly means
115 are derived from 10 different global climate models from the World Climate Research
116 (WCRP) Coupled Model Intercomparison Project (phase 3; CMIP3) and corrected by a
117 small equatorward bias [Fyfe and Saenko, 2006]. Changes in the wind fields include an
118 intensification of the maximum zonal wind stress by about 25% and a southward shift by
119 about 3.5° until 2100 [see Spence et al., 2010], as well as a southward shift of the boundary
120 between southern westerlies and trades in the tropics.

121 In order to differentiate between effects resulting from wind stress changes within the
122 meridional extent of the Southern Ocean westerlies and effects that modulate the trop-
123 ical trade winds, we include a second sensitivity experiment, posWIND, where only the
124 positive zonal (directed eastward) wind stress anomalies are added to the climatological

125 forcing. The resulting changes of the wind stress curl in experiment posWIND occur only
126 in the polar and subpolar region south of 40° S (Figure 1 b, red line).

3. Results

127 In response to anthropogenically induced global warming, the globally integrated marine
128 oxygen inventory of 256.6 Pmol simulated by experiment REF decreases by 4.8% until year
129 2100 (Figure 2a). This overall deoxygenation is damped by 15% in WIND and by 30% in
130 posWIND, such that average oceanic oxygen concentrations at the end of the simulation
131 remain higher in WIND and posWIND than in experiment REF. This can be explained by
132 the wind-driven increase of the MOC in experiments WIND and posWIND and associated
133 increase in the formation rate of oxygen-rich mode and intermediate water masses [Liu
134 and Wu, 2012; Downes et al., 2011] and deep water masses, which all represent important
135 pathways for the ventilation of the global ocean with oxygen.

136 The strengthening of the MOC is brought about by positive wind stress curl anomalies
137 applied in both WIND and posWIND simulations between 40° and 60° S (see Figure
138 1b). This is illustrated in Figure 2b-d by a deepening of the 20 Sv isoline of the zonally
139 integrated overturning stream function from ~1500m in REF to ~2500m in WIND and
140 posWIND. Note that the upwelling branch of the MOC is essentially identical in WIND
141 and posWIND because, in our model, the Southern Ocean upwelling is determined by the
142 strength and position of the westerlies.

143 Relative to the reference simulation, the formation rates of SAMW, AAIW and AABW
144 increase by about 40%, 50% and 30%, respectively, in the WIND experiment. For the
145 posWIND experiment, the formation rates increase by 20%, 50% and 70%, respectively.

146 The formation rates of the AAIW are directly linked to changes in the strength of the
147 westerlies, which are the same in WIND and posWIND. The shift of the boundary between
148 westerlies and trades (difference between WIND and posWIND) results in a stronger wind
149 stress curl anomaly between 40°S and 53°S in experiment WIND, which in turn yields a
150 larger increase in SAMW formation than in posWIND.

151 The response of AABW formation to the shift of the trades–westerlies boundary in
152 WIND is substantial (40% less than compared to posWIND). In both wind scenarios
153 the upwelling, which feeds both the AABW formation in the south and the mode and
154 intermediate water formation further north, is very similar. The northward transport of
155 surface waters from the polar front to the SAMW formation sites is, however, increased
156 by the wind shift of the trade-westerlies boundary in WIND compared to posWIND. The
157 combination of similar upwelling and increased surface water mass transport to the north
158 results in less southward supply to the AABW formation sites and thus in reduced increase
159 of AABW formation in WIND than in posWIND. The changes in the water mass tracers
160 (Figure 2b-c) illustrate that an increase in deep water formation is more important for
161 the global oxygen inventory than an increase in mode water formation.

162 Figure 3a shows the linear oxygen trend for the time period 1960–2010 at 300 m depth
163 for simulation REF. Contrary to the observed decrease in oxygen, but consistent with
164 earlier UVic model simulations [Stramma et al., 2012a], simulation REF yields slightly
165 increasing oxygen concentrations over large areas of the tropical thermocline including
166 the OMZ. Because simulation REF applies climatological wind fields, the changes in the

167 oxygen fields are solely driven by buoyancy changes that derive from anthropogenic- CO_2
168 induced temperature and salinity changes.

169 When, in addition to CO_2 emissions, changes in southern hemispheric wind fields are
170 applied in experiment WIND, the simulated increase in tropical oxygen concentrations
171 over the 1960–2010 time period becomes significantly smaller (Figure 3b). Applying only
172 the intensification of the southern westerlies in experiment posWIND (Figure 3c), the
173 oxygen trend is close to that of experiment REF. We conclude that the changes in trop-
174 ical ocean oxygen trends in experiment WIND are, at least for the time period 1960 to
175 2010, predominantly caused by the southward shift of the boundary between trades and
176 westerlies rather than by the intensification of the Southern Ocean westerlies.

177 The reduction in tropical thermocline oxygen levels in simulation WIND relative to
178 REF seems, at first sight, contradictory to the previously shown wind-induced increase
179 of the global oxygen inventory. However, the models' ideal age tracers reveal that it is
180 the strengthening and southward shift of the subtropical gyre circulation that leads to a
181 decrease of the northward transport of newly-ventilated oxygen-rich waters of subantarctic
182 origin along the eastern coast of the South Pacific into the OMZ: Figure 3d shows the ideal
183 age (colored contour) and the circulation (vectors) at 300m depth for REF, with the black
184 contour line denoting the equatorward boundary of the subtropical gyre circulation. A
185 southward shift of this boundary in response to the southern hemispheric wind anomalies
186 applied in WIND leads to a strengthening and a southward shift of the subtropical gyre
187 circulation and an increase in simulated ideal age north of this boundary (Figure 3e).
188 The increase in simulated ideal age north of 20°N amounts to up to 29 years in 2100

189 (Figure 3d-f). When the applied wind anomalies are restricted to the southern westerlies
190 in experiment posWIND, changes in the subtropical gyre circulation and in ideal age are
191 much reduced compared to those of the WIND simulation (Figure 3f).

192 To complete our analysis, we now investigate possible downstream effects of changes
193 in the formation rates of SAMW on the tropical oxygen minimum zone. In the steady-
194 state simulations of Palter et al. [2010], 30-60% of the water on the 26.8 isopycnal in
195 the EEP between 30°S and 30°N originate from SAMW (their Figure 6) and suggest
196 that the associated nutrient transport could be sensitive to climate change. In our model
197 experiments, SAMW also circulates northward from the formation area along the 26.8
198 isopycnal and we find a steady-state average contribution of $\sim 20\%$ between 30°S and
199 30°N, slightly lower than Palter et al. [2010]. In the EEP the 26.8 isopycnal is located
200 at a depth of approximately 280-310 m under pre-industrial conditions. Given that the
201 mean water age, derived from the ideal age tracer, in the suboxic waters of the EEP at
202 300 m depth is 276 years, we suggest that an increase of the Southern Ocean overturning
203 circulation does not have a large impact on the OMZ dynamics on time scales of 50
204 years (which is currently the time span covered by observations used to estimate oxygen
205 trends). Indeed, after 50 years only 5% of the newly formed SAMW reach the EEP in
206 our experiment. Since there is no significant difference in the depth of the 26.8 isopycnal
207 in the EEP between experiments REF and posWIND we conclude that planetary wave
208 processes forced remotely by a perturbation in the Southern Ocean can, to first order, be
209 neglected in the analysis of southern hemispheric wind impacts on the tropical OMZ.

210 The sensitivity to southern hemispheric wind anomalies is even larger for simulated
211 suboxic volume changes until the end of the 21st century. Figure 4 shows the suboxic
212 volume of the Pacific Ocean, here defined as water with oxygen concentrations smaller
213 than 10 mmol m^{-3} . In REF, we find an increase of the suboxic volume of $\sim 36\%$ until 2100.
214 Note that the suboxic volume expands already during 1960–2010, when all simulations still
215 show some local oxygen increase in the tropical thermocline (Figure 3a-c). Applying the
216 full southern-hemispheric wind anomalies in WIND results in an increase of the suboxic
217 volume twice as large as in REF (total increase of $\sim 72\%$), whereas a mere change of the
218 southern westerlies (posWIND) has negligible effect on suboxic volume changes compared
219 to experiment REF. This indicates that observed and expected 21st century changes in
220 the meridional extension of the tropical trade winds are as important for suboxic volume
221 changes as CO_2 -induced atmospheric heat flux changes of a business-as-usual emission
222 scenario.

4. Summary and Conclusion

223 In our study we investigate the impact of changes in the southern hemispheric wind
224 fields on global oxygen as well as on the extension of the tropical OMZ relative to changes
225 forced by CO_2 -induced atmospheric buoyancy flux changes only. The changes in the
226 southern hemispheric wind fields, which are in line with an observed shift of the SAM,
227 are a combination of a strengthening and poleward shift of the southern westerlies and a
228 poleward shift of the boundary between southern westerlies and tropical trade winds.

229 Our results confirm that the Southern Ocean plays an important role for the global
230 ocean oxygen supply. We show that a strengthening of the southern westerlies, that leads

231 to an increase of the water formation rates of the oxygen-rich deep and intermediate water
232 masses, can counteract part of the warming-induced decline in marine oxygen levels. The
233 wind-driven intensification of the Southern Ocean meridional overturning circulation in
234 both wind experiments leads to an increase in the global oxygen supply (Figure 2a). These
235 results indicate that changes in the formation of deep water are crucial for changes in the
236 global oxygen inventory. While the strength of the westerlies is identical in simulations
237 WIND and posWIND, the southward shift of the boundary between westerlies and trades
238 in WIND results in a larger increase of SAMW production and a smaller increase of deep
239 water formation and associated oceanic oxygen supply.

240 The southward shift of the boundary between westerlies and trade winds leads to an
241 intensification and a southward shift of the subtropical gyre circulation. Associated with
242 this is a decrease in northward water mass transport along the eastern margin into the
243 shadow zones of the subtropical gyre and thus into the OMZ. Our model simulations reveal
244 that changes in the meridional expansion of the tropical trade winds have a significant
245 impact on the evolution of the suboxic volume in the tropical OMZ during the 21st century:
246 The increase in suboxic volume in experiment WIND (72%) is twice as large as in the
247 buoyancy-only driven experiment REF (36%), whereas a mere change of the southern
248 westerlies, as in posWIND, does not alter the suboxic volume significantly with respect
249 to experiment REF.

250 Although the total change applied to the model's trade winds is small compared to the
251 climatological wind forcing, the impact on the 21st century OMZ dynamics is as large
252 as the impact of buoyancy driven changes forced by CO₂-induced atmospheric heat flux

253 changes alone. Our study thus illustrates the importance of realistic wind forcing for
254 adequate modeling of thermocline biogeochemical tracer distributions. Changes in the
255 meridional extension of the trade winds can also be driven by other processes, such as
256 changes in the Pacific Decadal Oscillation, ENSO or by local weather changes, which
257 are not necessarily restricted to the southern hemisphere and will have to be included in
258 future research.

259 **Acknowledgments.** The model data used to generate the figures will be available at
260 http://thredds.geomar.de/thredds/catalog_open_access.html.

261 This study was financially supported by BIOACID II and SFB754. We thank C.J. Somes
262 for proof-reading and three anonymous reviewers for their very constructive comments.

References

- 263 Bopp, L., Le Quéré, C., Heimann, M., Manning, and P. Monfray (2002), Climate-induced
264 oceanic oxygen fluxes: Implications for the contemporary carbon budget. *Global Bio-*
265 *geochemical Cycles*, 16, 2, 1022, doi:10.1029/2001GB001445.
- 266 Cai, W. (2006), Antarctic ozone depletion causes an intensification of the South-
267 ern Ocean super-gyre circulation, *Geophysical Research Letters*, Vol. 33, L03712,
268 doi:10.1029/2005GL024911
- 269 Deutsch, C., Berelson, W., Thunell, R., Weber, T., Tems, C., McManus, J., Crusius,
270 J., Ito, T., Baumgartner, T., Ferreira, V., Mey, J., van Geen, A. (2014), Centennial
271 changes in North Pacific anoxia linked to tropical trade winds, *Science*, 345 (665),
272 doi:10.1126/science.1252332

- 273 Dietze, H., Loeptien, U., 2013. Revisiting "Nutrient Trapping" in global biogeochemical
274 Ocean Circulation Models, *Global Biogeochem. Cy.*, 1-20, doi:10.1002/gbc.20029.
- 275 Downes, S. M., A. S. Budnick, J. L. Sarmiento, and R. Farneti (2011), Impacts of wind
276 stress on the Antarctic Circumpolar Current fronts and associated subduction, *Geophys.*
277 *Res. Lett.*, 38, L11605, doi:10.1029/2011GL047668.
- 278 Duteil, O., C. W. Böning, and A. Oschlies (2014), Variability in subtropical-tropical cells
279 drives oxygen levels in the tropical Pacific Ocean, *Geophys. Res. Lett.*, 41, 89268934,
280 doi:10.1002/2014GL061774.
- 281 Fanning, A.G., Weaver, A.J. (1996), An atmospheric energy-moisture model: Climatology,
282 interpentadal climate change and coupling to an ocean general circulation model. *J.*
283 *Geophys. Res.* 101: 15111 – 15128.
- 284 Fyfe, J.C., Saenko, O.A. , Zickfeld, K., Eby, M., Weaver, A.J. (2007), The Role
285 of Poleward-Intensifying Winds on Southern Ocean *J. Climate*, 20, 53915400. doi:
286 <http://dx.doi.org/10.1175/2007JCLI1764.1>
- 287 Fyfe, J.C., Saenko, O.A. (2006), Simulated changes in extratropical Southern Hemisphere
288 winds and currents. *Geophys. Res. Lett.*, 33, L06701, doi:10.1029/2005GL025332
- 289 Gent, P.R., McWilliams, J. (1990), Isopycnal mixing in ocean circulation models. *J. Phys.*
290 *Oceanogr.* 20, 150 – 155.
- 291 Getzlaff, J., Dietze, H. (2013) Effects of increased isopycnal diffusivity mimicking the
292 unresolved equatorial intermediate current system in an earth system climate model,
293 *Geophysical Research Letters*, 40 (10). pp. 2166-2170. DOI 10.1002/grl.50419

- 294 Keller, D. P., Oschlies, A., and Eby, M. (2012): A new marine ecosystem model for the
295 University of Victoria Earth System Climate Model, *Geosci. Model Dev.*, 5, 1195-1220,
296 doi:10.5194/gmd-5-1195-2012.
- 297 Liu, C., and L. Wu (2012), An intensification trend of South Pacific Mode Wa-
298 ter subduction rates over the 20th century, *J. Geophys. Res.*, 117, C07009,
299 doi:10.1029/2011JC007755.
- 300 Marshall, J., Speer, K. (2012) Closure of the meridional overturning circulation
301 through Southern Ocean upwelling *Nature Geoscience*, 5. pp. 171–180. DOI:
302 10.1038/NGEO1391
- 303 Marshall, G. J., 2003: Trends in the Southern Annular Mode from observations and
304 reanalyses. *J. Climate*, 16, 4134-4143.
- 305 Oschlies, A., K. G. Schulz, U. Riebesell, and A. Schmittner (2008), Simulated 21st centurys
306 increase in oceanic suboxia by CO₂-enhanced biotic carbon export, *Global Biogeochem.*
307 *Cycles*, 22, GB4008, doi:10.1029/2007GB003147.
- 308 Pacanowski, R. C., 1995. MOM 2 Documentation, User's Guide and Reference Manual.
309 Tech. Rep. 3, GFDL Ocean Group.
- 310 Palter. J.B., Sarmiento, J.L., Gnanadesikan, A., Simeon, J., Slater, R.D. (2010), Fuel-
311 ing export production: nutrient return pathways from the deep ocean and their de-
312 pendence on the Meridional Overturning Circulation, *Biogeoscience*, 7, pp. 3549–3568.
313 DOI: 10.5194/bg-7-3549-2010
- 314 Ridder, N. and England, M.H. (2014), Sensitivity of ocean oxygenation to variations
315 in tropical zonal wind stress magnitude, *Global Biogeochem. Cycles*, 28, 909926,

- 316 doi:10.1002/2013GB004708.
- 317 Ridgway, K. and Hill, K.. 2009. Chapter 5: The East Australian Current. In: Marine
318 Climate Change in Australia 2009: Impacts and Adaptation Responses. pp. 52-64.
319 NCCARF, Queensland. ISBN 978-1-921609-03-9
- 320 Roemmich, D., Gilson, J., Davis, R., Sutton, P., Wijffels, S., Riser, S. (2007), Decadal
321 Spinup of the South Pacific Subtropical Gyre. *J. Phys. Oceanogr.*, 37, 162173. doi:
322 <http://dx.doi.org/10.1175/JPO3004.1>
- 323 Saenko, O. A., Fyfe, J.C., England, M.H. (2005), On the response of the oceanic wind-
324 drive circulation to atmospheric CO₂ increase, *Climate Dynamics*, 25, pp. 415–426.
325 DOI: 10.1007/s00382-005-0032-5
- 326 Spence, P., Fyfe, J. C., Montenegro, A., Weaver, A. J. (2010), Southern Ocean Response to
327 Strengthening Winds in an Eddy-Permitting Global Climate Model, *Journal of Climate*,
328 23, pp. 5332–5343
- 329 Stramma L., Oschlies, A., Schmidtko, S. (2012a), Mismatch between observed and mod-
330 eled trends in dissolved upper-ocean oxygen over the last 50 yr, *Biogeosciences*, 9, 4045
331 – 4057, DOI: 10.5194/bg-9-4045-2012
- 332 Thompson, D.W.J. and Solomon, S. (2002), Interpretation of Recent Southern Hemisphere
333 Climate Change, *Science* 296, 895 (2002);DOI: 10.1126/science.1069270
- 334 Weaver, A.J., Eby, M., Wiebe, E. C., et al. (2001), The UVic earth system climate model:
335 Model description, climatology, and applications to past, present and future climates,
336 *Atmos. Ocean*, 39, 361 – 428.



Figure 1. a) Zonal average of monthly zonal wind stress anomalies in Pa applied in the model simulations. b) Zonal average of the annual mean wind stress curl anomaly for experiments WIND (blue) and posWIND (red) in year 2100.

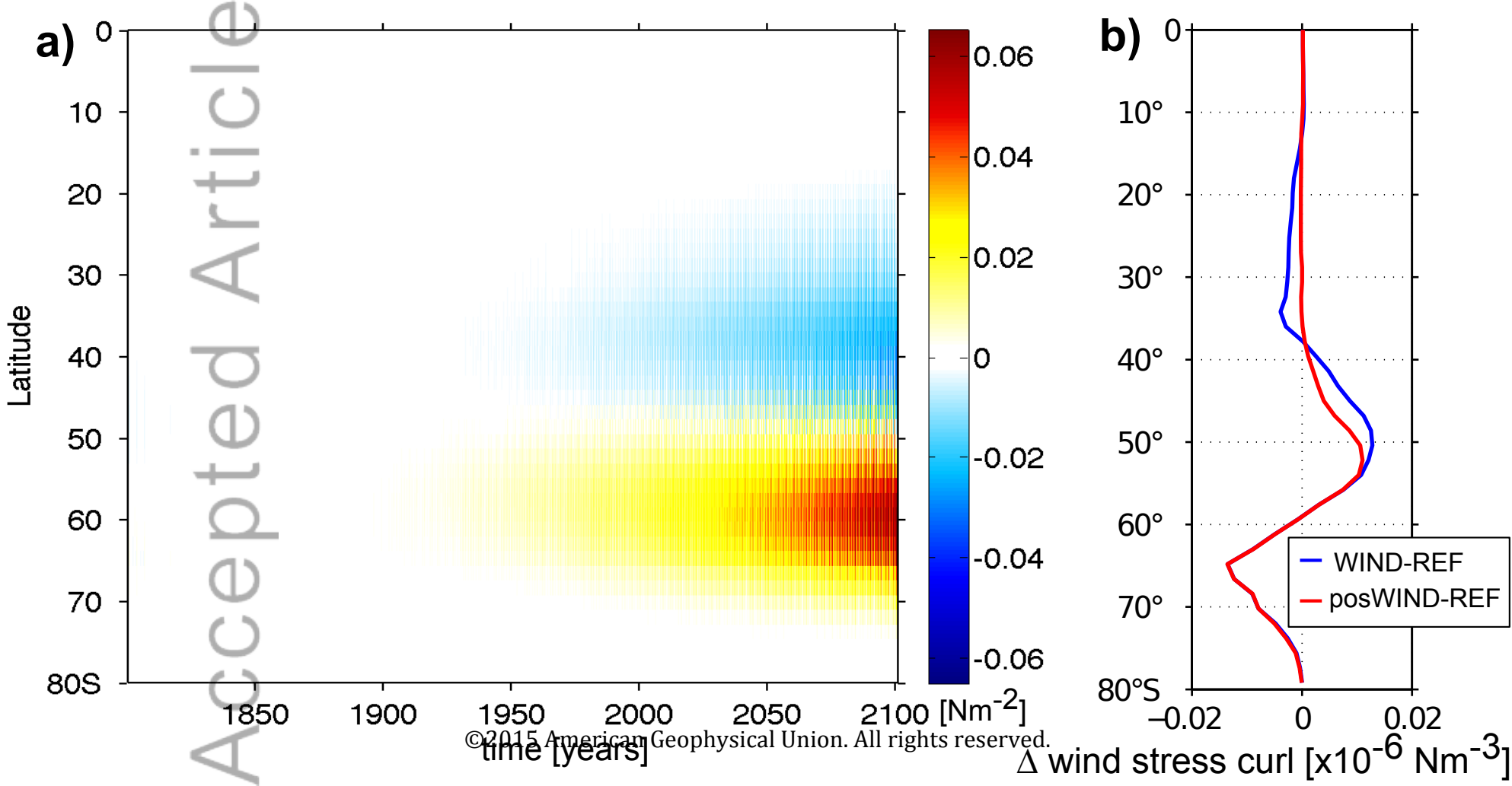
Figure 2. a) Global oxygen inventory in Pmol. The bottom panels show the simulated Eulerian Southern Ocean meridional overturning in Sv in year 2100 (contour): b) REF, c) WIND and d) posWIND. In b) the colored background shows the distribution of the sum of the zonally averaged idealized SAMW and AABW tracers in % in REF for year 2100, c-d) show the differences in % for WIND-REF and posWIND-REF, respectively, for the sum of the zonally averaged idealized SAMW and AABW tracers.

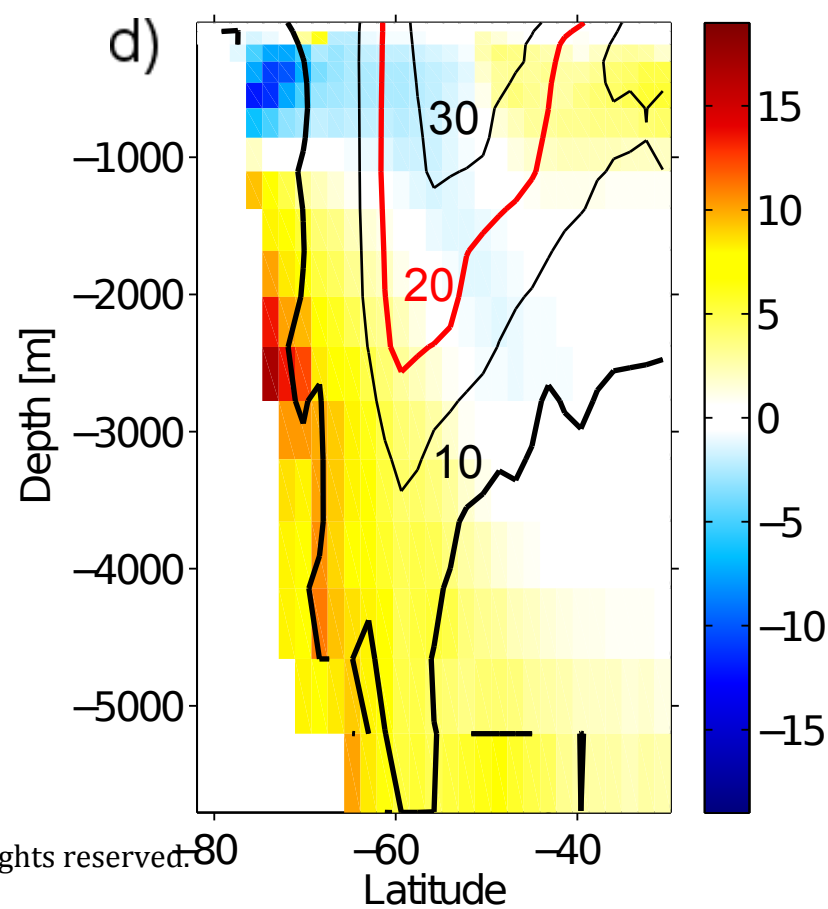
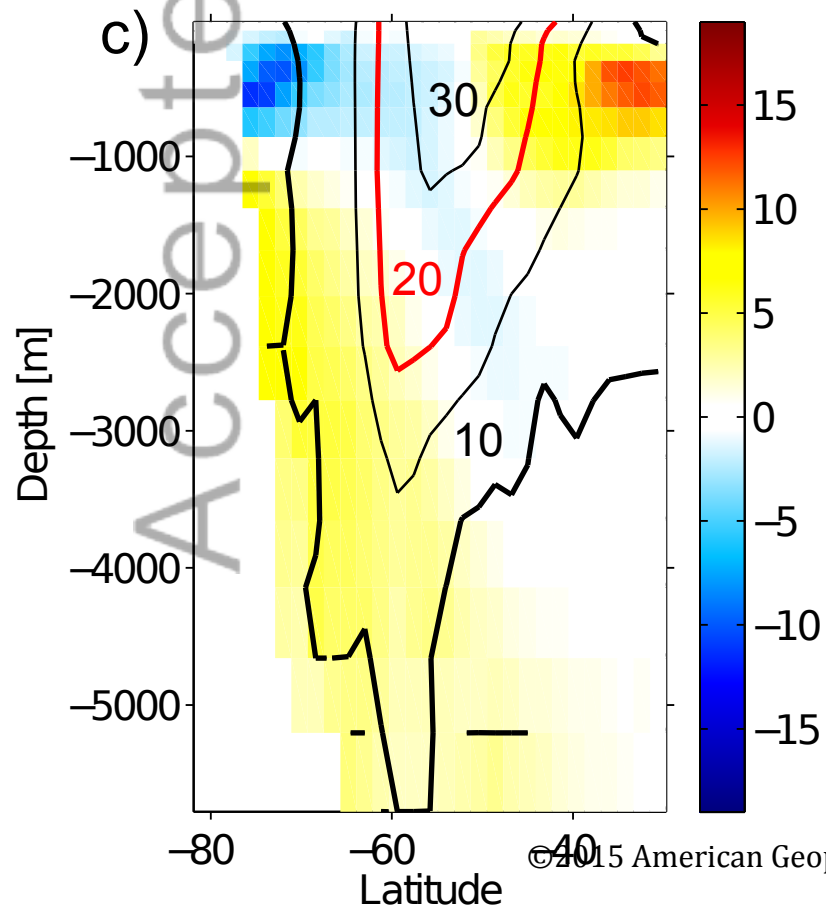
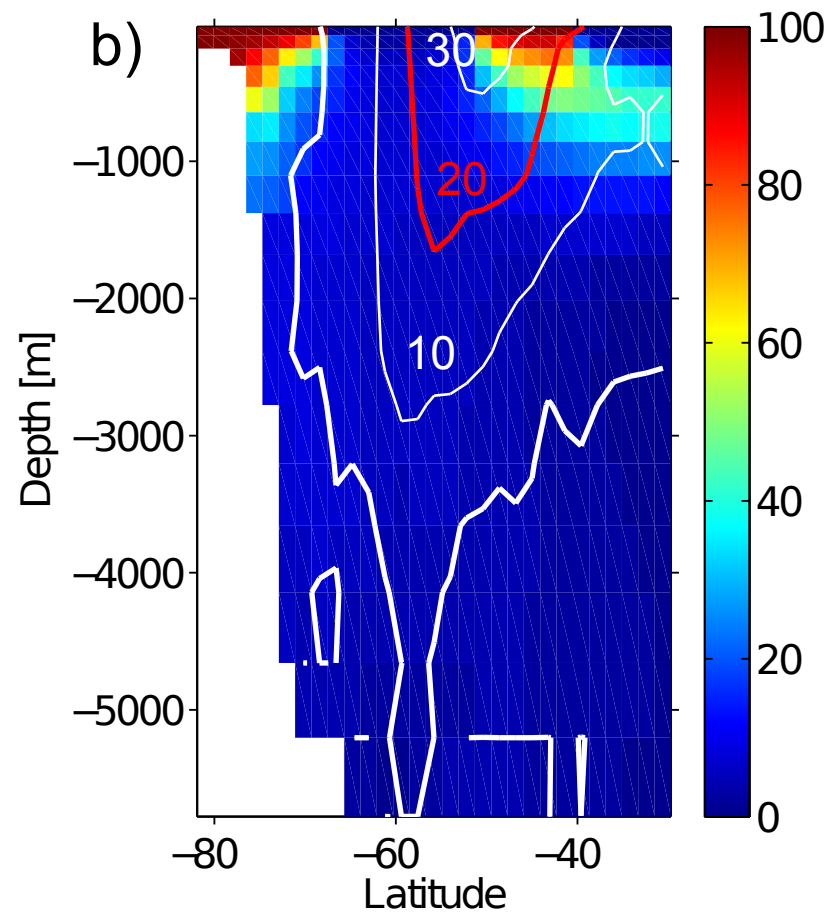
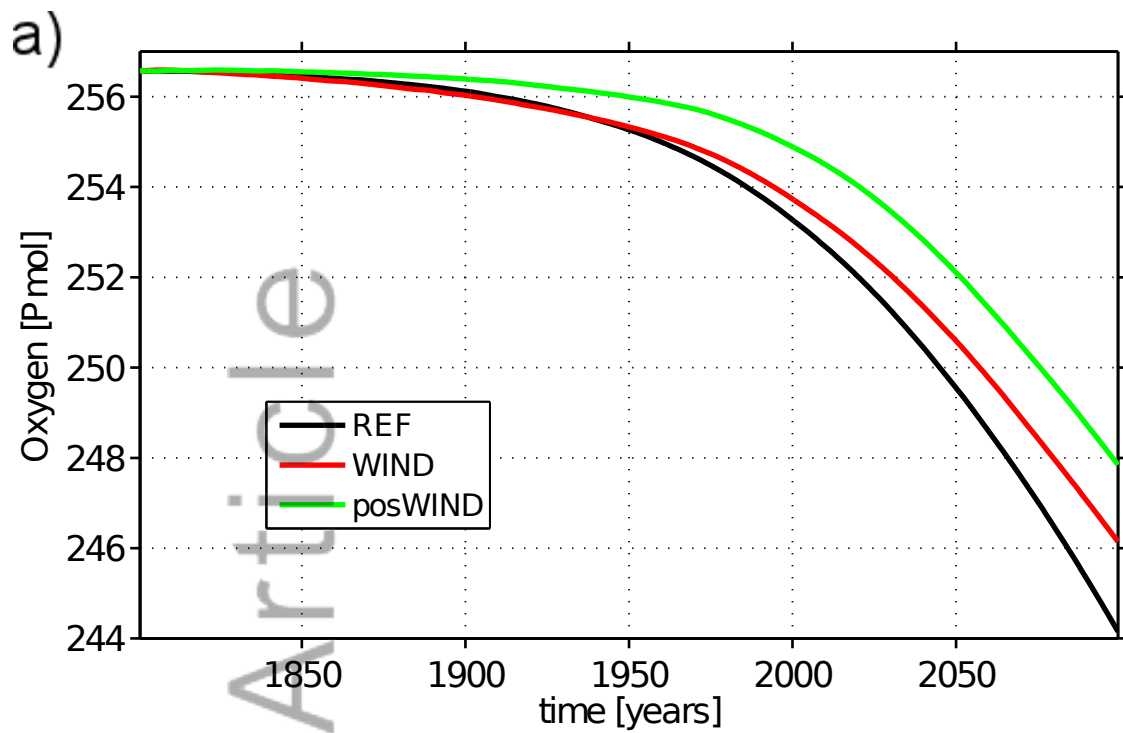
Accepted Article

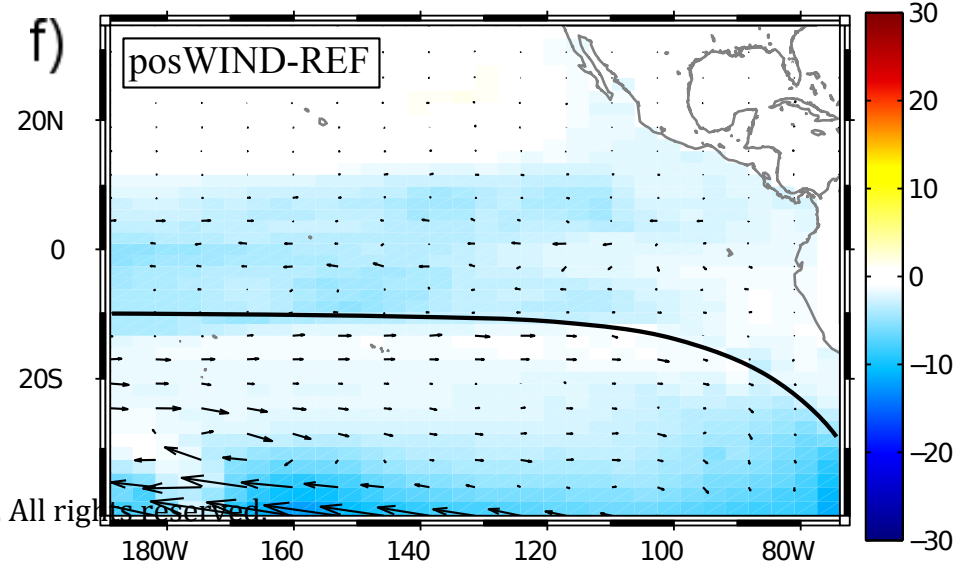
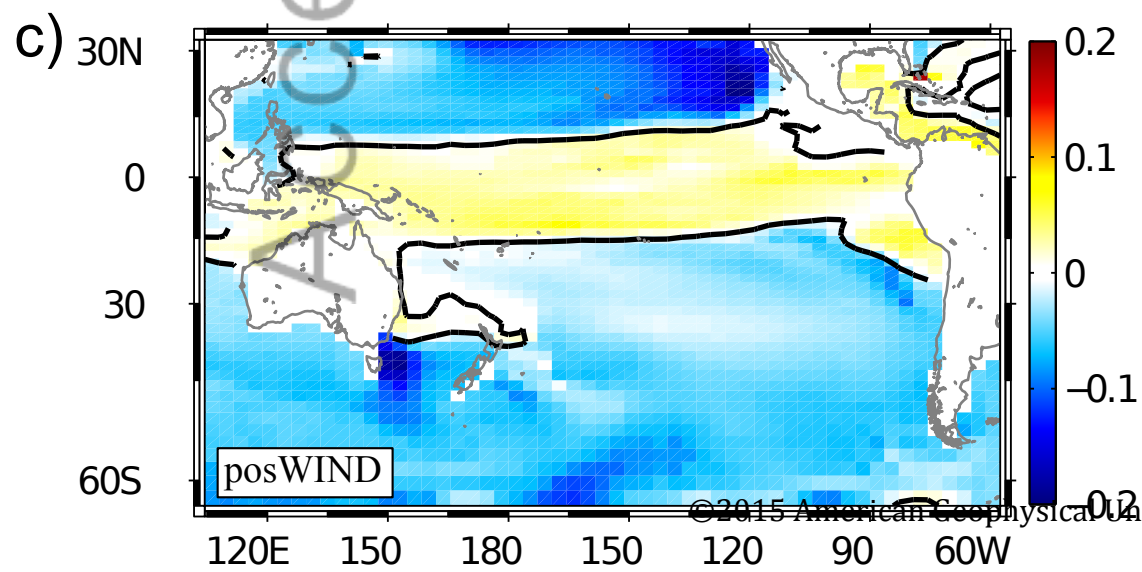
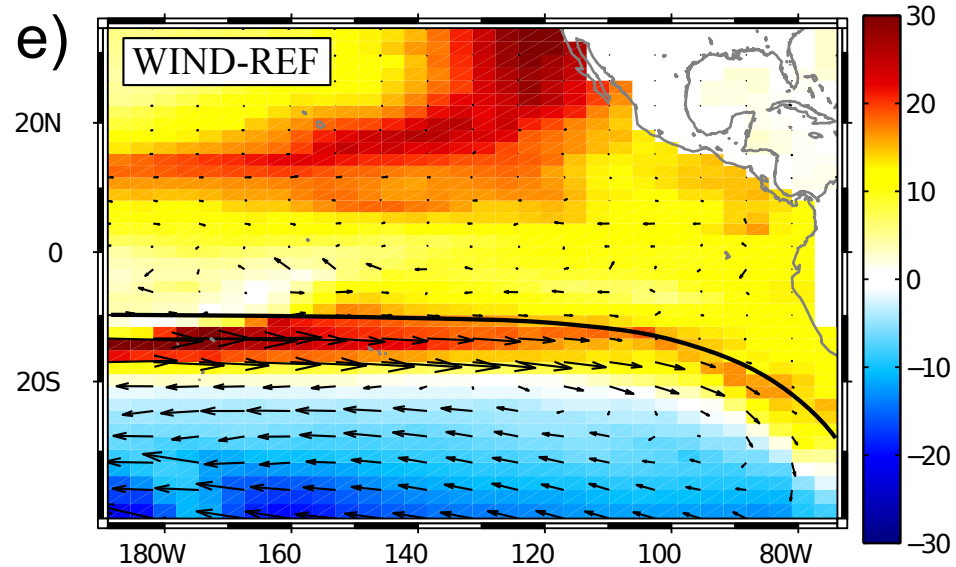
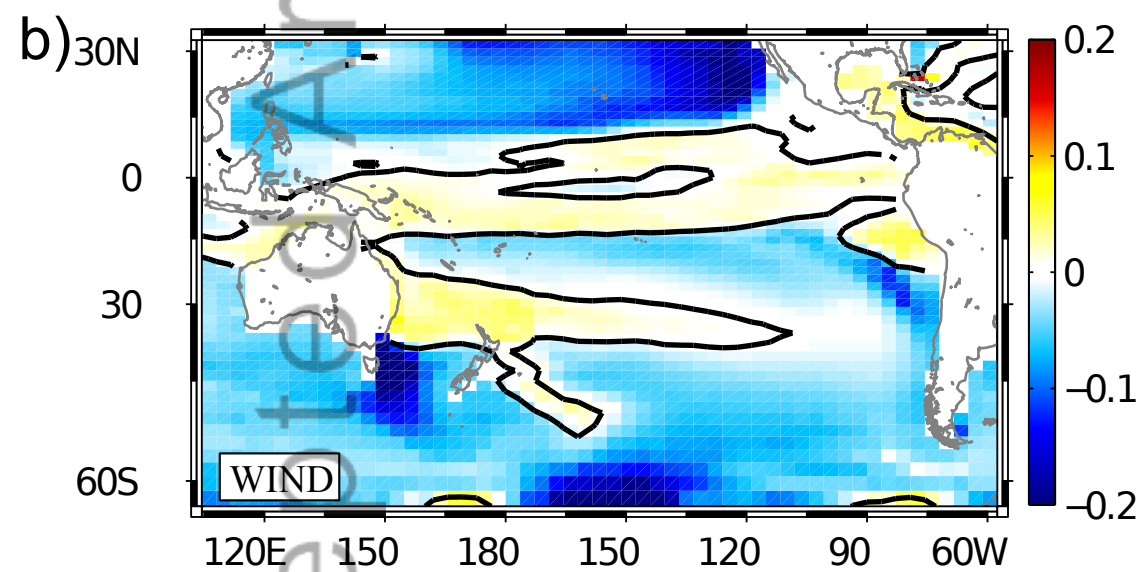
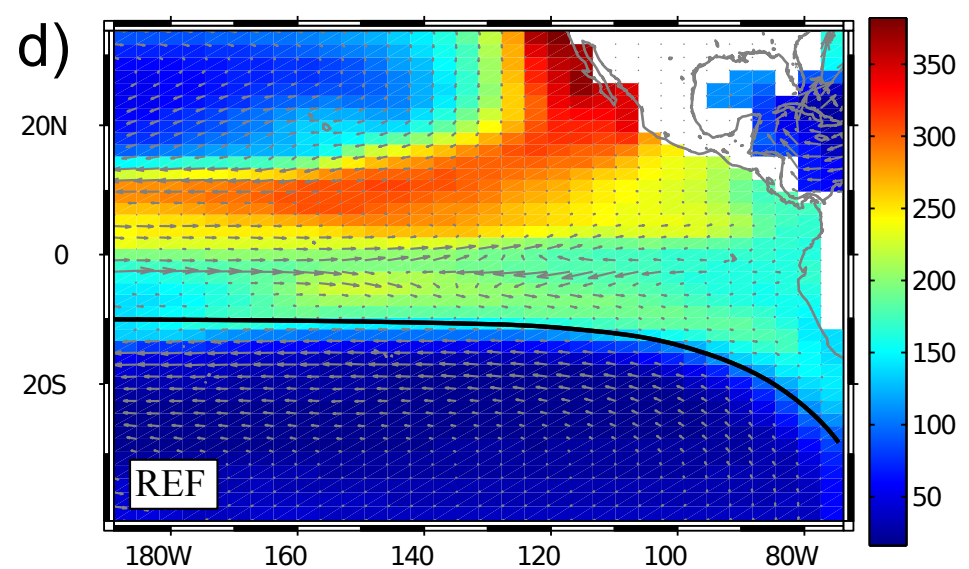
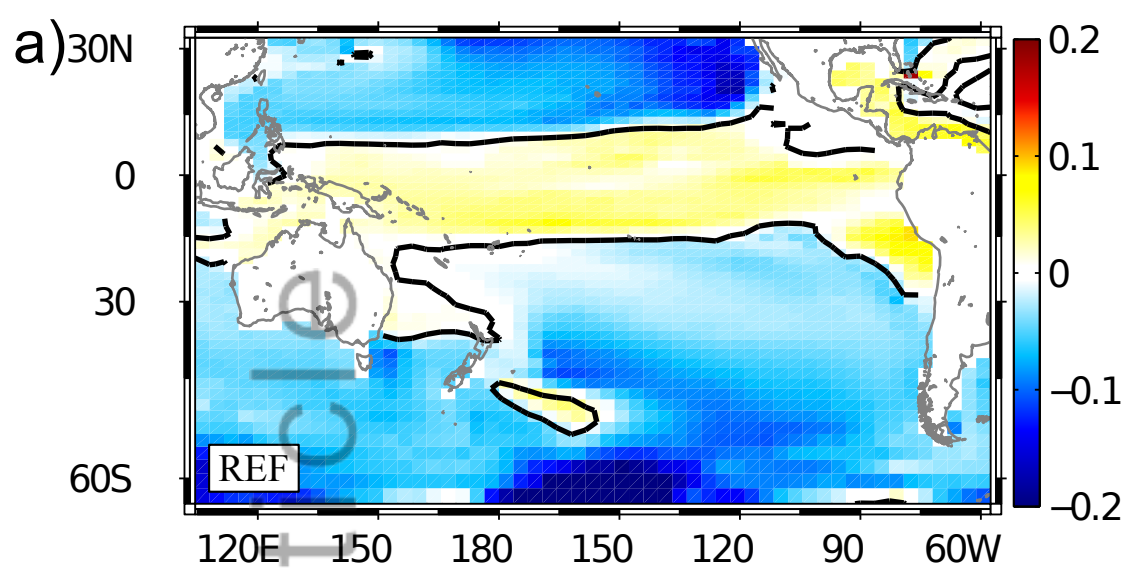


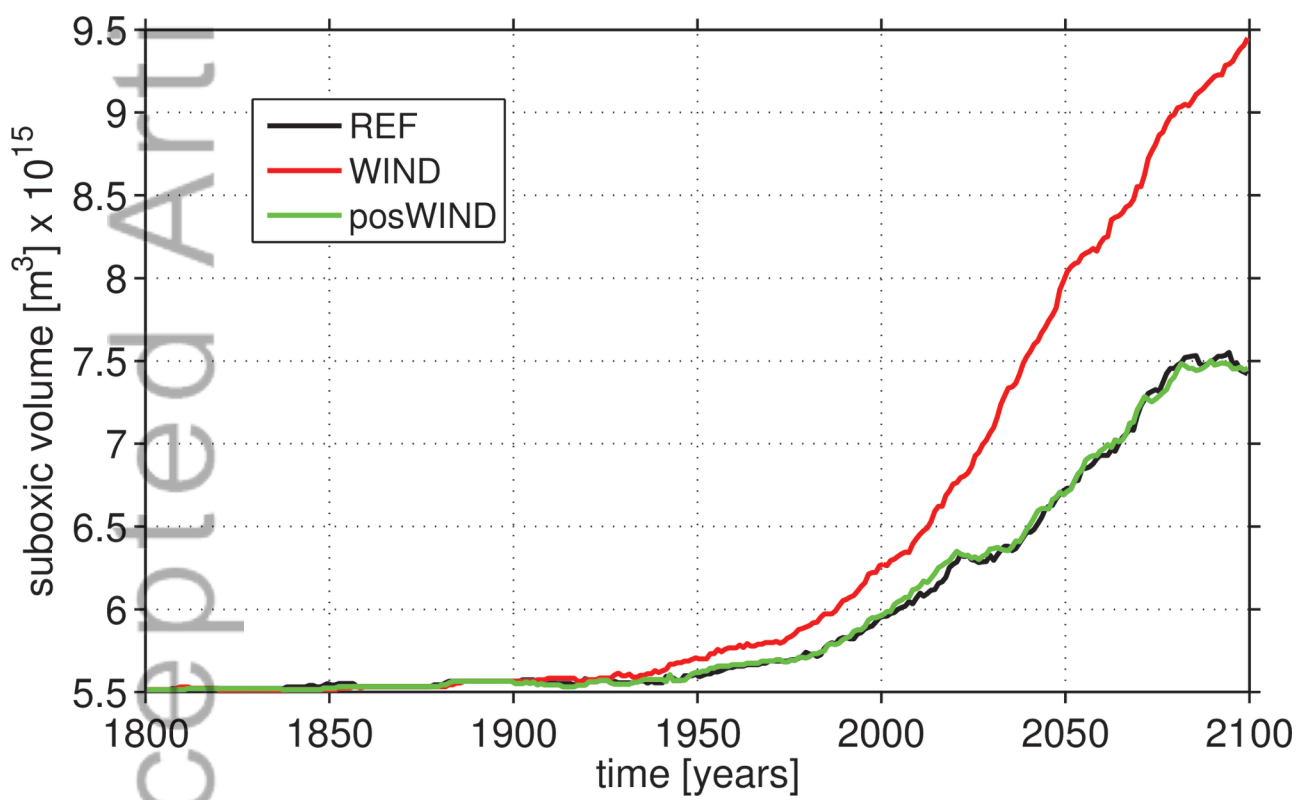
Figure 3. The left-hand panels show the oxygen trend ($\text{mmol m}^{-3} \text{year}^{-1}$) at 300 m depth for 1960–2010 a) REF, b) WIND and c) posWIND. Negative trends indicate a decrease in oxygen. The right-hand panels show the ideal age in years and velocity vectors at 300 m depth in year 2100 for d) REF, e) difference WIND-REF and f) difference posWIND-REF. Positive values in b) and c) indicate a larger ideal age. The black contour line is the same in all three panels and shows the equatorward boundary of the subtropical gyre in REF, here defined as the location with zero zonal velocity.

Figure 4. Simulated suboxic volume [m^3] of the Pacific Ocean, defined as water hosting $\text{O}_2 < 10 \text{ mmol m}^{-3}$, as a function of time.









2015gl066841-f03-z-